

Bonding Corneal Tissue: Applications of Photoactivated Diazopyruvoyl Cross-linking Agent

George T. Timberlake*^{1,2}, Abraham L. Yousef¹, Stacy R. Chiles¹, Rachel A. Moses¹ and Richard S. Givens^{1,2}

¹Department of Chemistry, University of Kansas, Lawrence, KS

²Department of Ophthalmology, University of Kansas Medical Center, Kansas City, KS

Received 6 February 2005; accepted 5 May 2005; published online 9 May 2005 DOI: 10.1562/2005-02-06-RA-433

ABSTRACT

Photoactivated bis-diazopyruvamide—N,N'-bis(3-diazopyruvoyl)-2,2'-(ethylenedioxy)bis(ethylamine), (DPD)—was previously shown to bond materials containing type I collagen. However, tensile strength of bonded collagenous tissue (~78% water) was low compared with that of dehydrated collagenous gelatin (~14% water). Here we investigated the role of water in corneal tissue bond strength and in bonding corneal tissue to glass. Bonding corneal tissue to glass may be of value in surgically anchoring keratoprotheses to corneas to alleviate problems with extrusion. Bovine corneal samples were lyophilized for various times resulting in tissue hydrations of zero (no water content) to ~3.7 (normal water content). The lyophilized corneal tissue was bonded to solid gelatin sheets, to other corneal samples and to glass using 0.3M DPD in chloroform. Control runs used chloroform only. Samples were irradiated with 100 or 200 J of 320–500 nm light. Strong bonds formed with all three materials when corneal tissue hydration was ≤1. No bonds or extremely weak bonds formed when tissue hydration levels were >1. No bonding occurred with chloroform alone. Formation of strong bonds only occurs with hydration levels ≤1 because corneal collagen fibrils are tightly packed and close enough to cross-link with the 1.78 nm long DPD.

INTRODUCTION

Sutures are used in ocular surgery to attach donor corneal buttons to recipient corneas in corneal transplantation (penetrating keratoplasty), to seal incisions for intraocular lens implant after cataract extraction, to close scleral incisions and wounds and occasionally to flatten wrinkled corneal flaps after LASIK. Although modern suture materials and techniques are largely successful in ocular wound repair, a number of suture-related problems remain, particularly in corneal surgery. For example, approximately 25% of penetrating keratoplasty grafts experience suture complications including

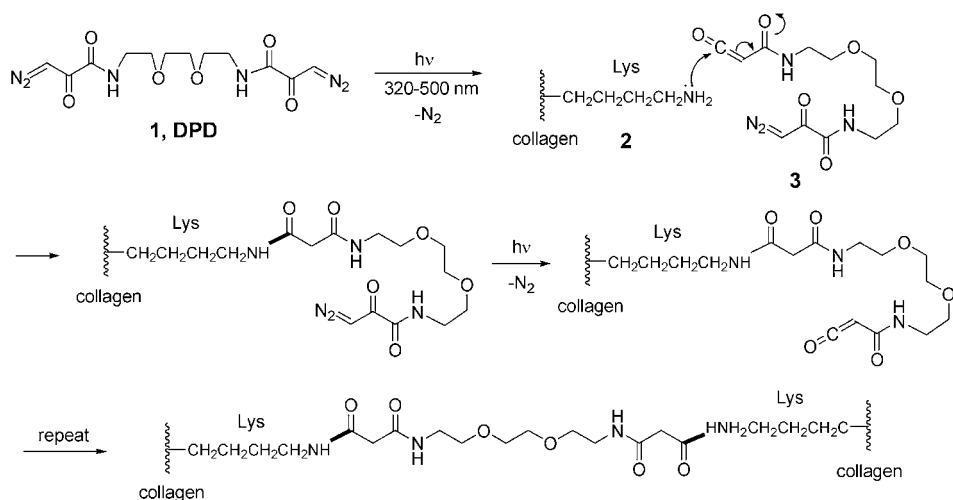
exposed sutures, abscesses, breakage and loosening and wound dehiscence (1). Corneal sutures can also act as sites of inflammation, stimulating blood vessel growth into the normally avascular cornea (2). Eroded or broken sutures may also result in infection in sutured corneoscleral incisions for intraocular lens implantation (3).

These problems with corneal sutures have driven the search for alternative means of wound closure. Several photochemical protein cross-linking methods of corneal wound closure have been explored. Kochevar and colleagues (4–7) have used the photosensitizer rose bengal and 514 nm laser irradiation to seal full-thickness corneal incisions and penetrating keratoplasties in rabbits (6). The exact mechanism of wound closure is not known, but it is thought that reactive species produced by irradiation react by forming covalent cross-links with proteins such as collagen through electron donors such as tryptophan, tyrosine and cysteine. Judy and colleagues (8–12) synthesized a bifunctional light-activated tissue-bonding reagent based on two photoactivatable 1,8-naphthalimide groups covalently bound by a polyethylene chain or “tether.” One form of this class of bifunctional reagents, MBM Gold, has been tested in bonding *ex vivo* human corneal stroma (12).

We have designed and synthesized a tethered bis-diazopyruvamide reagent N,N'-bis(3-diazopyruvoyl)-2,2'-(ethylenedioxy)bis(ethylamine) (DPD) (1, Scheme 1) for ocular wound closure that cross-links type I collagen, possibly through bond formation with nucleophilic centers such as the primary amine groups on lysine and hydroxylysine (13) (2, Scheme 1). α -Diazoketones lose nitrogen upon heating to 80–90°C (14,15) or with light irradiation and subsequently undergo a Wolff rearrangement to produce reactive ketenes that are susceptible to nucleophilic attack from amines and other nucleophiles (16). In previous experiments (13) DPD successfully bonded rabbit Achilles tendon, but the bonds were relatively weak compared with bonds of type I collagen in dehydrated gelatin sheets (“gel strips”). Gel strips, however, are relatively dehydrated compared with fresh tissue (14% vs 78% water, respectively). Thus, the strength of tissue bonds with DPD may be affected by the high water content. Specifically, the photoactivated DPD ketene (3, Scheme 1) will react with endogenous nucleophiles including the primary amines in lysine and hydroxylysine and the aqueous environment surrounding the collagen triplex. It is possible that unproductive water-to-DPD bonds weaken overall tissue bond strength. The strength of tissue bonds may also be adversely affected by the spacing of collagen fibrils, which is much larger than the length of the DPD molecule (1.78 nm) in both tendon and cornea.

* To whom correspondence should be addressed: Department of Ophthalmology, University of Kansas Medical Center, Kansas City, KS 66160-7379, USA. Fax: 913-381-7726; e-mail: gtimberl@kumc.edu
Abbreviations: AFM, atomic force microscopy; DPD, N,N'-bis(3-diazopyruvoyl)-2,2'-(ethylenedioxy)bis(ethylamine).

© 2005 American Society for Photobiology 0031-8655/05

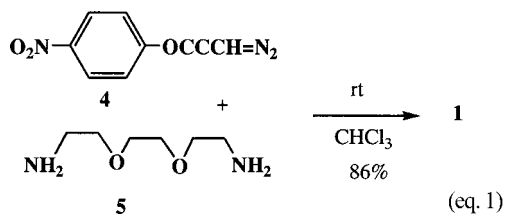


Scheme 1. Lysine groups on neighboring collagen polypeptides are cross-linked through DPD.

To investigate these issues we examined bovine corneal stromal bonding with fully hydrated tissue and tissue with varying degrees of dehydration. The cornea consists of an exterior cellular layer (the epithelium), an interior layer of collagen and matrix (the stroma) and an interior cellular layer (the endothelium). The stroma is rich in type I collagen fibrils that are evenly spaced at approximately 36 nm and surrounded by an aqueous interfibrillar matrix. We hypothesized that removing water from the tissue would decrease unproductive reactions with H₂O and that collagen fibrils would move closer together, increasing the likelihood of more extensive cross-linking by DPD. We attempted to measure the change in collagen fibril spacing resulting from dehydration by imaging corneal collagen using atomic force microscopy (AFM) because AFM does not require special tissue processing such as that used for transmission electron microscopy that could distort collagen fibril morphology. We also explored bonding corneal tissue to glass to test the feasibility of bonding solid, biocompatible materials such as keratoprotheses (artificial corneal lenslets) or glaucoma filtration valves to ocular tissue. Bonding to glass is possible because some glasses have nucleophilic hydroxyl groups at their surfaces that can be derivatized or attached directly to other functional groups. Here we report the results of experiments in bonding corneal tissue to gel strips, to other corneal tissue and to glass.

METHODS

Synthesis of DPD. The diazopyruvamide was synthesized from reaction of *p*-nitrophenyl-3-diazopyruvate (16) (**4**, Eq. 1) with 2,2'-(ethylenedioxy)bis(ethylamine) (**5**, Eq. 1) under anhydrous conditions. The detailed steps of the synthesis are described in an earlier paper (13).



Gel strips. Bovine gelatin sheets (Shionogi Qualicaps, Inc., Whitsett, NC) were washed in ethanol to remove dust, fingerprints

and other surface impurities. The sheets were cut into 0.5 × 2.5 cm strips and stored until needed.

Bovine cornea. Corneas were dissected from ~2 h postmortem bovine eyes. Epithelial and endothelial cell layers were removed by scraping. Corneas were cut into two strips, each ~5 × 15 mm. Each strip was then cut in half parallel to the corneal surface using a fine scalpel. The two resulting strips were weighed and placed stromal side up on glass slides, covered with another slide, and dehydrated in a vacuum lyophilizer for various amounts of time. Lyophilized corneal samples were weighed again to determine the extent of dehydration before use in experiments. For irradiation and bonding, one sample was placed stromal side up on a quartz slide. The other sample (gel strip, cornea or glass) was placed on top, forming an overlap area of ~5 × 5 mm. Two μL of the bonding reagent (0.3M DPD in CHCl₃) was instilled between the two samples and another quartz slide placed on top. Light fingertip pressure was applied evenly to the quartz slides that sandwiched the samples, which were then held in place with small clamps.

Irradiation was carried out using a Novacure 2000 near-UV light source (Exfo, Missisagua, Ontario, Canada) as described previously (13). Samples were placed in the diverging beam from the liquid light guide at a position where beam diameter was 3.8 cm. External filters provided a net transmission of 80% in the 320–500 nm range, and 0% below 320 nm and above 550 nm. Light power in the central 6 × 6 mm of the light beam where the tissue was placed (an area slightly larger than the area of sample overlap) was ~0.25 W, giving a power density of ~0.7 W/cm². Exposure time (typically 400–480 s) was adjusted to produce an exposure of 100 J for cornea-to-gel-strip and cornea-to-glass bonds. Due to light scattering by lyophilized corneal samples, the exposure for cornea-to-cornea bonds was doubled (200 J). The quartz glass slides holding the samples for irradiation were slightly warm to the touch after irradiation, approximately 40–45°C, much less than the 80–90°C required for Wolff rearrangement in α-Diazoketones (14,15). However, to rule out the possibility that this modest heating could initiate the Wolff rearrangement, a sample of DPD (12 mg, 0.035 M) was dissolved in chloroform-d (1 mL) and heated at 50°C in the dark in an oil bath. No change was detected in the ¹H NMR spectrum after 1 h of heating. Saturation of the solution with deuterated water and further heating of the sample at 50°C for an additional 20 min also produced no detectable change in the NMR spectrum.

Tensile testing was carried out as described previously (13). Briefly, one side of the bond (tissue, gel strip or glass) was clamped to the screw-driven crosshead of a tensiometer. The other side of the bond was clamped to a stationary strain gauge. As the screw turned, the crosshead moved, gradually increasing the force on the bond. The force was transduced by the strain gauge and the stress-strain curve recorded using an A/D converter and computer.

In separate experiments, the water content of corneal tissue was determined by extensive lyophilization (>12 h) and found to be 78.5% ($N = 31$, $sd = \pm 5.5\%$). Hydration of corneal samples was calculated using the method of Fratzl and Daxer (17),

$$H = (P/P_0) - 1$$

where H is the hydration, P is the tissue mass at hydration H , and P_0 is the mass of the completely dehydrated tissue. We estimated the completely dehydrated tissue mass, P_0 , using the previously measured tissue water content (78.5%). Thus, $P_0 \approx (1 - 0.785) \times P$.

Contact mode AFM was performed using a Digital Instruments (Santa Barbara, CA) model LFM-2 atomic force microscope and CSD 12/50 contact silicon cantilevers (MikroMasch, Portland, OR).

RESULTS

Cornea-to-gel-strip bonding. Bonding cornea to gel strips was tested first because gel-strip bonding has been well characterized in our initial studies with DPD (13) and therefore serves as a model bonding substrate. The tensile strength of corneal stroma-to-gel strip bonds depended strongly on the hydration level of the corneal sample. Figure 1 shows stress-strain plots of two bonded samples with different levels of hydration. The maximum (breaking) stress for the more dehydrated sample ($H = 0.34$) was 70 N/cm² (Fig. 1A); the less dehydrated sample ($H = 1.96$) ruptured at 6 N/cm² (Fig. 1B). The low hydration level sample (Fig. 1A) did not exhibit a plastic region in the stress-strain curve, indicative of a brittle bond; the high hydration level sample (Fig. 1B) exhibited plastic regions near the maximum stress point. We observed that more hydrated corneal samples partially dissolved the gel strips, possibly contributing to the plastic region. Maximum stresses for all 21 samples tested are shown in Fig. 1C as a function of the hydration level of the corneal sample. Corneal stroma-to-gel-strip bonding was relatively weak (≤ 10 N/cm²) when the tissue hydration level was greater than 1. When the hydration level was less than 1, however, greater bond strengths were observed (10–74.7 N/cm²), but bond strengths were variable. Control samples irradiated with the solvent (CHCl₃) alone failed to produce any bonds.

Cornea-to-cornea bonding. Like cornea-to-gel-strip samples, cornea-to-cornea bond strength depended on the level of tissue hydration. Relatively dehydrated ($H < 1$) samples often exhibited high maximum stresses (up to 46.5 N/cm²) and brittle bonds that broke with relatively little movement of the tensiometer crosshead (Fig. 2A). Higher levels of hydration ($H > 1$) had lower maximum stresses (most often < 10 N/cm²), exhibited plastic regions near maximum stress and required greater crosshead movement to rupture (Fig. 2B). Maximum breaking stress as a function of hydration level for all 17 samples tested is shown in Fig. 2C. The two bonded corneal samples usually had somewhat different hydration levels, shown by circles and squares (Fig. 2C). High tensile strength bonds were only achieved with tissue hydration levels less than 1. Control samples with chloroform alone failed to produce any bonding.

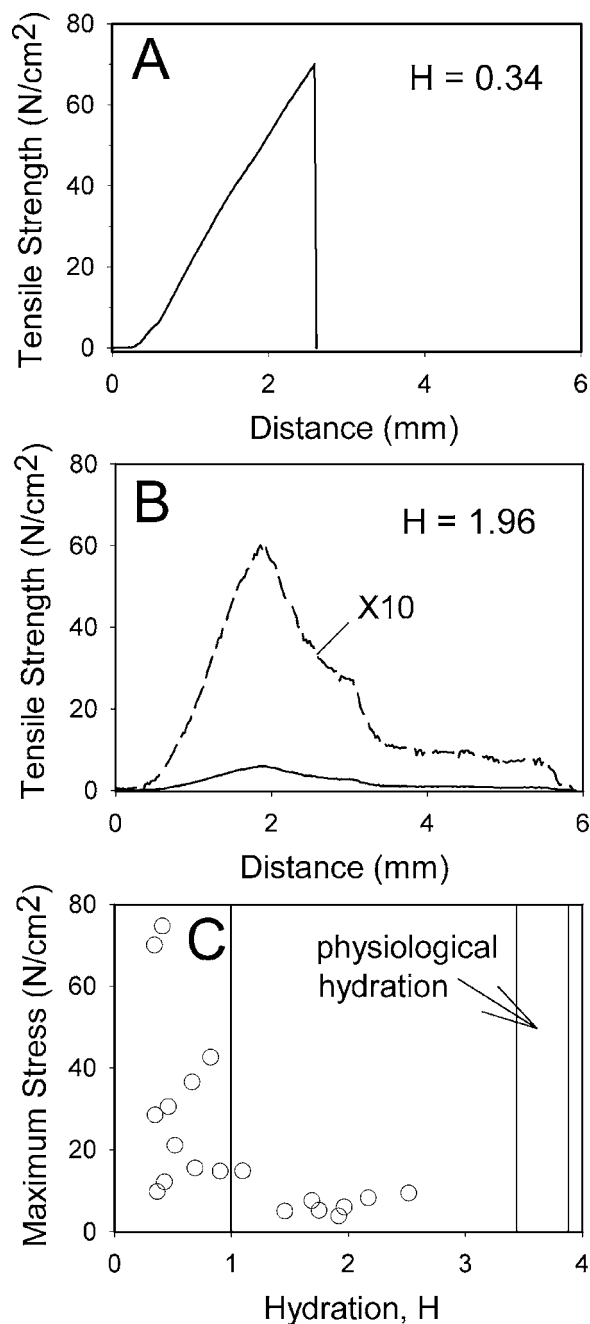


Figure 1. Corneal stroma-to-gel-strip bonds. A: Stress-strain plot of highly dehydrated corneal sample. H is the corneal tissue hydration value. B: Solid line: stress-strain plot of relatively hydrated sample. Dashed line: 10 \times magnification of solid line. C: Maximum stress for 21 cornea-to-gel-strip bonds. Two vertical lines on right correspond to 78.5% \pm 1% water content, the physiological hydration range of corneal tissue.

Gel-strip-to-glass and cornea-to-glass. Bonding to glass was first tested with gel strips. The mean bond strength was quite high, 65.8 N/cm², and exceptionally strong bonds (> 90 N/cm²) were achieved. Having demonstrated that materials containing type I collagen (gel strips) can be bound to glass, corneal samples were bonded to glass using 0.3 M DPD in CHCl₃. Bond stress-strain characteristics and tensile strength depended on the level of tissue hydration. Figure 3A shows a stress-strain curve for a corneal sample with $H = 0.22$ exhibited high maximum stress (33.9 N/cm²)

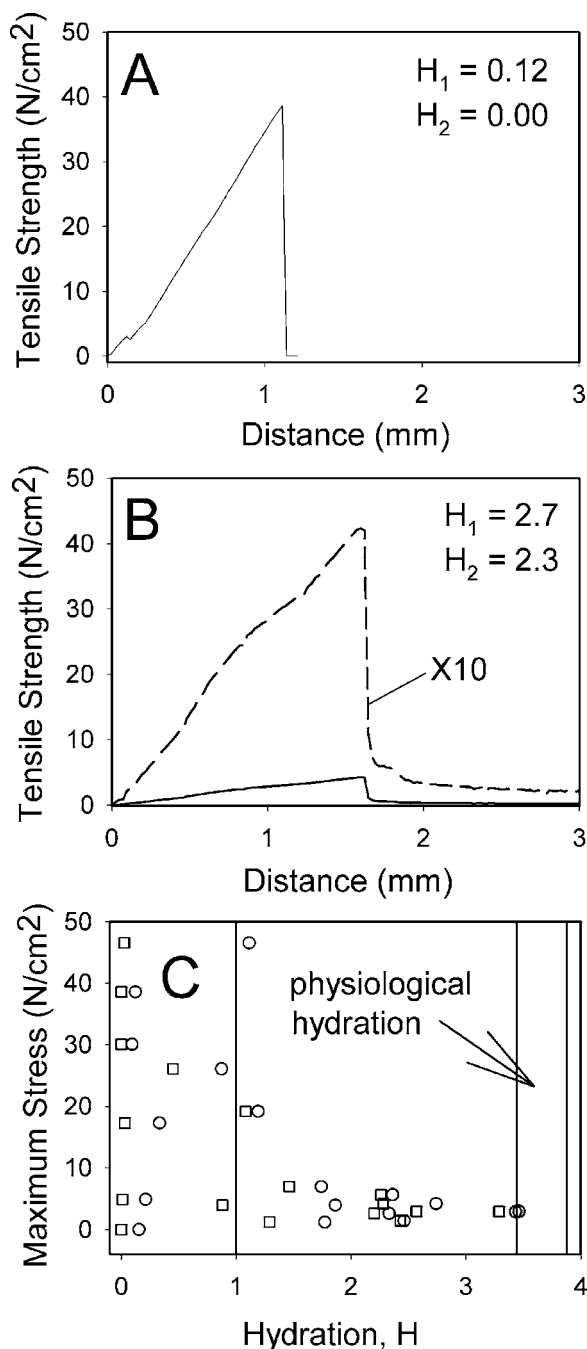


Figure 2. Corneal stroma-to-corneal stroma DPD bonds. A: Stress-strain curve of bonded corneal samples with hydration levels <1 . Maximum stress = 39 N/cm^2 . H_1, H_2 : hydrations of the two corneal samples. B: Solid line: stress-strain curve of bonded samples with hydration levels >1 . Dashed line: $10\times$ magnification of solid line. Maximum stress = 4.2 N/cm^2 . C: Maximum stresses of all 17 sample pairs as a function of hydration level, H . Squares (\square) = lower level and circles (\circ) = higher level of hydration of each pair.

and the brittle characteristics seen with gel strip and cornea-to-cornea bonds. The strongest bond of all samples with $H > 1$ was 3.4 N/cm^2 for a sample of hydration $H = 1.82$ (Fig. 3B). All other samples with $H > 1$ failed to produce any bond. Maximum stresses for all 24 samples tested are shown in Fig. 3C. Strong bonds were formed only when tissue hydration levels were <1 although there

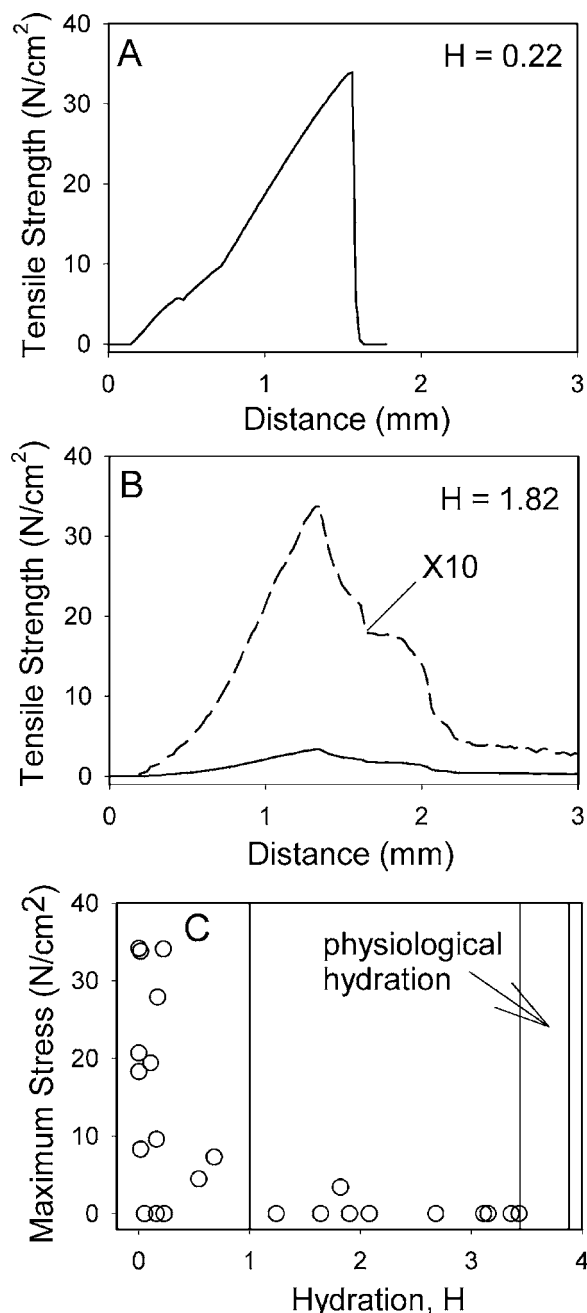


Figure 3. Glass-to-corneal stroma bonds. A: Stress-strain curve of relatively dehydrated corneal sample. B: Solid line: stress-strain curve of a sample with a relatively high level of hydration. Dashed line: $10\times$ magnification of solid line. C: Maximum stress as a function of the level of tissue hydration for all 24 samples tested. 0.3 M DPD in CHCl_3 .

were four samples with hydration levels <1 that failed to form any bond. Control bonds with CHCl_3 produced no bond.

Atomic force microscopy. Exposed stromal surfaces of corneal tissue samples were examined by AFM in an effort to determine how the spacing between collagen fibrils changed with dehydration. It was only possible, however, to image fully dehydrated samples because the AFM deflection tip broke or was entrapped when there was water in the sample. Fibrils appear to be confluent (Fig. 4), but this could be due in part to artifactual broadening of the fibrils by an AFM tip that was large relative to the fibrils. Fully dehydrated

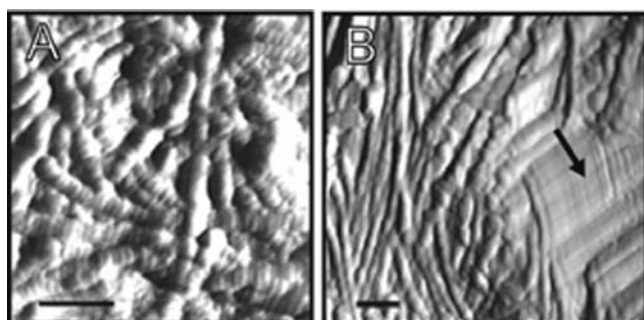


Figure 4. Atomic force microscopy images of fully dehydrated corneal stroma. A: Disorganized fibrils. B: Both disorganized and organized (arrow) fibrils. Bars: 250 nm.

samples exhibited bare collagen fibrils parallel to the exposed stromal surface. Areas of random fibril arrangement (Fig. 4A) as well as areas of parallel arrangement (arrow Fig. 4B) were observed.

DISCUSSION

The results described above demonstrate that DPD can strongly bond corneal stromal tissue to itself, to other collagenous materials (gel strips) and to glass. Shear strengths as high as 46.5 and 74.7 N/cm² were achieved for corneal stroma-to-stroma bonding and cornea-to-gel-strip bonding respectively. These values exceed those reported by Judy *et al.* (11) for rabbit skin (~8 N/cm²) and human meniscus (9) (~17 N/cm²) at comparable energy densities. It is not possible to compare the present tensile strengths to those of Kochevar *et al.* (4,5) because they measured bursting pressure for corneal bonds and peeling tensile strength for skin bonds.

The major finding of this study is that strong tissue bonds (>10 N/cm²) are only formed when corneal tissue hydration is ~1 or less. This finding is understandable in terms of a model of corneal stromal dehydration proposed by Fratzl and Daxer (17). Using synchrotron x-ray diffraction, these investigators found that collagen fibril diameter remained constant (36 nm) as tissue was dehydrated from physiological levels down to $H = 1$. Below that point, fibril diameter decreased linearly with further dehydration, reaching a diameter of 26 nm for $H = 0$. They propose a two-phase model of dehydration based on biochemical and ultrastructural findings (18,19) that fibrils have bound proteoglycans that form a proteoglycan/water “coating” around the fibril, increasing its diameter to 36 nm.

The Fratzl and Daxer (17) model is illustrated graphically in Fig. 5. Initially, corneal collagen fibrils with their proteoglycan coats are spaced in an even hexagonal array and are separated from one another by about the 36 nm fibril diameter (20,21) (Fig. 5B). As corneal tissue dehydrates from physiological levels, water is first lost from the interfibrillar matrix, causing the 36 nm diameter fibrils to move closer to one another (Fig. 5C). At hydration 1, interfibrillar water is gone, and water in the proteoglycan fibril coating begins to be removed (Fig. 5D). Finally, as hydration 0 is approached, only the “bare” fibrils remain (Fig. 5E) and at some hydration near 0, they are close enough for the 1.78 nm DPD molecules to connect to one another (Fig. 5F). Our finding that strong bonding occurs at hydrations of 1 or less suggests that DPD cross-links between collagen molecules in different fibrils can take place only when the water fibril “coating” begins to decrease and bare fibrils are abutted. Inasmuch as the DPD molecule is only 1.78

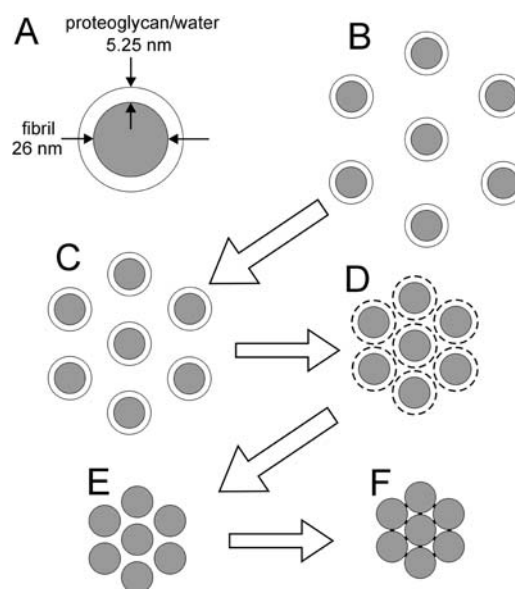


Figure 5. Illustration of model of corneal stromal dehydration proposed by Fratzl and Daxer (17). Collagen fibrils and DPD drawn to scale. A: Dimensions of corneal collagen fibril with proteoglycan-water coating. B: Hexagonal arrangement of collagen fibrils at physiological hydration ($H \approx 3.3$). C: Fibrils become closer as tissue dehydrates. D: Proteoglycan-water coat begins to disappear at $H = 1$. E: Bare collagen fibrils closer with further dehydration. F: Collagen fibrils separated by 1.78 nm, the DPD molecular length.

nm in length, abutted bare (or almost bare) fibrils might be required for fibril-to-fibril bonds.

AFM of the stromal surface of fully dehydrated corneal samples revealed bare collagen fibrils in both random and parallel arrangements in different areas. This structure should maximize the opportunity for DPD fibril cross-linking because the bare fibrils of one sample are pressed against those of the other sample, putting fibrils in close enough proximity for cross-linking by the 1.78 nm DPD molecule. We could not determine whether bare fibrils were present at higher hydrations due to AFM limitations, but this seems unlikely given the findings of Fratzl and Daxer (17).

Strong bonding of corneal stroma to glass demonstrates the possibility of sutureless attachment of appliances such as keratoprotheses to the cornea. Keratoprotheses are small lenses that are surgically inserted through the central cornea when the cornea has become opaque due to disease and corneal transplants are not possible (22). The lenticular shape focuses incoming light onto the retina, providing the patient with vision that he or she would otherwise not have. A variety of plastic keratoprotheses have been manufactured and applied surgically. Although modern keratoprotheses are retained in the cornea for fairly long times (23), they can be extruded. Anchoring keratoprotheses with a light-activated bond such as DPD might keep the prosthesis in place for longer times.

To explore the possibility of DPD-anchored keratoprotheses, we used model keratoprotheses made of borosilicate glass (Fig. 6A). The diameter of the “stem” of the keratoprosthesis was 6 mm. Using a biopsy punch, a 6 mm hole was punched in the center of a full-thickness, dehydrated bovine cornea from which the epithelium had been removed. The keratoprosthesis was then inserted into the hole and pressed tightly against the dehydrated corneal surface and 5 μ L of 0.3 M DPD in CHCl₃ was applied

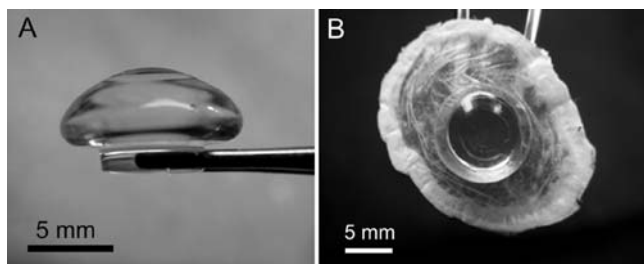


Figure 6. A: Model glass keratoprosthesis. B: Model keratoprosthesis bonded to dehydrated bovine cornea.

around the cornea–glass junction. The DPD was applied to seven corneal samples and the solvent (CHCl_3) alone was applied to an additional seven control samples. The keratoprosthesis and cornea were irradiated as described above for an exposure of 100 J. Figure 6B shows an example of a model keratoprosthesis bonded to a bovine corneal sample. Following irradiation, a connector was attached to the front (lens) surface of the keratoprosthesis with cyanoacrylate glue. The keratoprosthesis was mounted in a holder that held the cornea tightly but allowed the keratoprosthesis to move. A lightweight cup was then attached to the connector glued to the keratoprosthesis. Small weights were then gradually added to the cup until the keratoprosthesis pulled free of the cornea to which it was attached. It was not possible to measure the bonded area as we did previously, hence tensile strengths in N/cm^2 could not be calculated. The cornea-to-glass contact and bonding areas were approximately the same for all samples, however, so we simply measured the breaking force. The mean breaking force of DPD-bonded corneal samples (2.18 ± 1.42 N) was statistically significantly stronger (*t*-test: $t = 2.598$, $P = 0.023$) than the breaking force of control samples (0.66 ± 0.62 N).

In summary, we have found that our photoactivated collagen bonding agent, DPD, produces strong corneal tissue bonds with dehydrated tissue. This is most likely due to the short length of the DPD molecule relative to the spacing of corneal collagen fibrils in hydrated tissue and also to the hydrophobic nature of the reagent. To overcome the bonding limitations obtained with hydrated tissue, longer, more highly functionalized tethers, such as amine-functionalized dendrimers, will be necessary. Diazopyruvyl poly(amidoamine) dendrimers may address this problem, a strategy we are now exploring.

The ability of DPD to bond corneal tissue to glass, however, warrants further exploration due to the need to anchor appliances such as keratoprostheses or glaucoma filtration valves to ocular tissue. It may be possible to dehydrate the tissue in a highly local area, allowing implantation of glass prostheses without dehydrating large amounts of tissue. Finally, glass may not be an optimal choice for such bonding; certain plastics that have polyamine surfaces or glass coatings of alkyl groups terminating in primary amines would provide exposed nucleophilic centers that could serve as possible candidates for bonding with these reagents.

Acknowledgements—Supported by grants from the Kansas Lions Sight Foundation (GTT & RSG) and the NSF-REU Grant EEC-0139645. We are grateful to Mr. Cory Watson of Shinogi Pharmaceuticals for kindly providing the gelatin sheets. We wish to thank Mr. Matt Bichelmeyer of Bichelmeyer Meats, Kansas City, KS for providing bovine eyes.

REFERENCES

- Williams, K. A., D. Roder, A. Esterman, S. M. Muehlberg and D. J. Coster (1992) Factors predictive of corneal graft survival: report from the Australian Corneal Graft Registry. *Ophthalmology*, **99**, 403–414.
- Dana, M.-R., D. A. Schaumberg, V. O. Kowal, M. B. Goren, C. J. Rapuano, P. R. Laibson and E. J. Cohen (1995) Corneal neovascularization after penetrating keratoplasty. *Cornea*, **14**, 604–609.
- Cameron, J. A. and A. Huaman (1994) Corneoscleral abscess resulting from a broken suture after cataract surgery. *J. Cataract Refract. Surg.*, **20**, 82–83.
- Mulroy, L., J. Kim, I. Wu, P. Scharper, S. A. Melki, D. T. Azar, R. W. Redmond and I. E. Kochevar (2000) Photochemical keratodesmos for repair of lamellar corneal incisions. *Invest. Ophthalmol. Vis. Sci.*, **41**, 3335–3340.
- Chan, B. P., I. E. Kochevar and R. W. Redmond (2002) Enhancement of porcine skin graft adherence using a light-activated process. *J. Surg. Res.*, **108**, 77–84.
- Proaño, C. E., D. T. Azar, M. C. Mocan, R. W. Redmond and I. E. Kochevar (2004) Photochemical keratodesmos as an adjunct to sutures for bonding penetrating keratoplasty corneal incisions. *J. Cataract. Refract. Surg.*, **30**, 2420–2424.
- Proaño, C. E., L. Mulroy, E. Jones, D. T. Azar, R. W. Redmond and I. E. Kochevar (2004) Photochemical keratodesmos for bonding corneal incisions. *Invest. Ophthalmol. Vis. Sci.*, **45**, 2177–2181.
- Judy, M. M., J. L. Matthews, R. L. Boriack, A. Burlacu, D. E. Lewis and R. E. Utecht (1993) Photochemical cross-linking of proteins with visible-light-absorbing 1,8-naphthalimides. *SPIE Proc.*, **1882**, 305–308.
- Judy, M. M., H. Nosir, R. W. Jackson, J. L. Matthews, D. E. Lewis, R. E. Utecht and D. Yuan (1996) Bonding of human meniscal and articular cartilage with photoactive 1,8-naphthalimide dyes. *SPIE Proc.*, **2671**, 251–255.
- Judy, M. M., R. W. Jackson, H. R. Nosir, J. L. Matthews, J. D. Loyd, D. E. Lewis, R. E. Utecht and D. Yuan (1997) Healing results in meniscus and articular cartilage photochemically welded with 1,8-naphthalimide dyes. *SPIE Proc.*, **2970**, 257–260.
- Judy, M. M., H. Nosir, R. W. Jackson, J. L. Matthews, R. E. Utecht, D. E. Lewis and D. Yuan (1998) Photochemical bonding of skin with 1,8-naphthalimide dyes. *SPIE Proc.*, **3195**, 21–24.
- Timberlake, G. T., P. V. Mitrev, M. M. Judy, H. Nosir and J. L. Matthews (1997) Corneal laser welding using a light-activated, protein-crosslinking dye. *Invest. Ophthalmol. Vis. Sci. (ARVO Suppl.)*, **38**, S510.
- Givens, R. S., G. T. Timberlake, P. G. Conrad, A. L. Yousef, J. F. Weber and S. Amslinger (2003) A photoactivated diazopyruvyl cross-linking agent for bonding tissue containing type-I collagen. *Photochem. Photobiol.*, **78**, 23–29.
- Heyes, G. and G. Holt (1973) Thermal rearrangement of α -Dialkoxy- β -diketones. *J. Chem. Soc., Perkin I.* 1206–1209.
- Tomioka, H., N. Hayashi, T. Asano and Y. Izawa (1983) Mechanism of the photochemical and thermal Wolff rearrangement of 2-Dialkoxy-1,3-dicarbonyl compounds. *Bull. Chem. Soc. Jpn.*, **56**, 758–761.
- Goodfellow, V. S., M. Settineri and R. G. Lawton (1989) p-Nitrophenyl 3-diazopyruvate and diazopyruvamide, a new family of photoactive cross-linking bioprobes. *Biochemistry*, **28**, 6346–6360.
- Fratzl, R. and A. Daxer (1993) Structural transformation of collagen fibrils in corneal stroma during drying. *Biophys. J.*, **64**, 1210–1214.
- Craig, A. S., J. G. Robertson and D. A. D. Parry (1986) Preservation of corneal collagen fibril structure using low-temperature procedures for electron microscopy. *J. Ultrastruct. Mol. Res.*, **96**, 172–175.
- Scott, J. E. (1988) Proteoglycan-fibrillar collagen interactions. *Biochem. J.*, **252**, 313–323.
- Hogan, M. J., J. A. Alvarado, and J. E. Weddell (1971) *Histology of the Human Eye*. pp. 86–89. W. B. Saunders Co., Philadelphia.
- Meek, K. M., N. J. Fullwood, P. H. Cooke, G. F. Elliott, D. M. Maurice, A. J. Quantock, R. S. Wall and C. R. Worthington (1991) Synchrotron x-ray diffraction studies of the cornea, with implications for stromal hydration. *Biophys. J.*, **60**, 467–474.
- Doane, M. G., C. H. Dohlman and G. Bearse (1996) Fabrication of a keratoprosthesis. *Cornea*, **15**, 179–184.
- Dohlman, C. H. and M. G. Doane (1994) Some factors influencing outcome after keratoprosthesis surgery. *Cornea*, **13**, 214–218.